ASTRONOMY & ASTROPHYSICS
SUPPLEMENT SERIES

Astron. Astrophys. Suppl. Ser. 130, 235–244 (1998)

Millimetric Lunar Laser Ranging at OCA (Observatoire de la Côte d'Azur)

E. Samain[1], J.F. Mangin[1], C. Veillet[2], J.M. Torre[1], P. Fridelance[1], J.E. Chabaudie[1], D. Féraudy[1], M. Glentzlin[1], J. Pham Van[1], M. Furia[1], A. Journet[1], and G. Vigouroux[1]

[1] Observatoire de la Côte d'Azur, CERGA, Av. N. Copernic, F-06130 Grasse, France
e-mail: samain@obs-azur.fr
[2] CFHT, 65-1238 Mamalahoa Hwy, Kamuela HI 96743, U.S.A.

Received June 23; accepted November 27, 1997

Abstract. The Lunar Laser Ranging station at the Observatoire de la Côte d'Azur, France, permits to measure the Earth-Moon distance with millimetric precision. Applications in astronomy, lunar science, geodesy, and gravitation are summarised. Expected scientific results with millimetric Lunar Laser Ranging data are presented. A complete error budget is given, showing that the precision is mainly limited by the orientation and the size of the corner cube arrays placed on the Moon. The measurement accuracy is degraded by the bad knowledge of the air index. The time stability, computed from the lunar echoes, permits to extract the real precision of the Earth-Moon distance and to optimise the integration time of the normal points.

Key words: moon — gravitation — time instrumentation: miscellaneous

1. Introduction

In 1969, during the Apollo XI mission, the astronauts placed on the Moon the first corner cube array permitting to measure the Earth-Moon distance with the laser ranging technique. As early as in 1970, some Earth-Moon distances have been obtained with a precision in the 25 cm range at the McDonald laser station (Texas). Four other retroreflector arrays have been placed during the following Apollo XIV and XV, and Lunakhod 1 and 2 missions Faller 1972); (Chang et al. 1972); (Fournet 1972). McDonald was the only laser station ranging to the Moon on a routine basis for many years starting from 1970. In France, some lunar echoes were obtained at Pic du Midi Observatory in 1970. In 1984, two additional laser stations were built, one in Hawaii, the other in France, whereas the McDonald station came to a stop and was replaced by a smaller one. The French station, located at the Observatoire de la Côte d'Azur (OCA), is dedicated to Earth-Moon measurements. Its precision, in the 15 cm range at the beginning, reached the centimetre level in 1987 (Veillet 1987); (Veillet et al. 1993). The principle of Lunar Laser Ranging (LLR) is based on time propagation measurements of a light pulse between the Earth and the Moon. The start time of a laser pulse sent in the direction of the Moon is measured. A lunar retroreflector returns a fraction of the incident photons to the telescope and the return time is measured. The time interval between the start and return times permits to deduce the distance between the telescope and the retroreflector array, if the propagation velocity of the light pulses is known. In 1992, a millimetric Lunar Laser Ranging project started at OCA. This program aimed to improve both precision and accuracy of the OCA Lunar ranging station by one order of magnitude. Since 1995, observational results have been obtained with these "millimetric" performances (Samain 1995). After a brief review of the (LLR) scientific applications, we present the instrumental configuration of the station, the complete error budget and the current precision, and accuracy limitations.

2. Applications of lunar laser ranging

Lunar laser ranging has many applications in various domains including astronomy, lunar science, geodynamics, and gravitational physics (Dickey et al. 1994); (Nordvedt 1996); (Williams et al. 1996). In astronomy, LLR data are used to build lunar ephemeris relying only on these data. The millimetric data provide a determination of radial distance variations with 6 mm accuracy and can improve the angular-rate and the mean distance uncertainties. LLR

Send offprint requests to: E. Samain

data contribute to planetary ephemeris and are essential for the positioning of these ephemeris in the fundamental astronomical reference frame at the milliarcsecond level. Ephemerides are used for spacecraft navigation and mission planning, and for every precise astronomical computation such as reference frame connection or asteroid mass determination.

The study of LLR data provides a lot of information concerning the dynamics of the Moon: the gravitational harmonics, the moments of inertia and their differences, the lunar Love number k_2, and variations in the lunar physical librations. As these values are related to the composition of the Moon, we can deduce the mass distribution, the internal dynamics, and obtain information on the Moon's structure. The Love number k_2 measures the tidal changes in the moments of inertia and gravity. The apparent k_2 obtained from LLR analysis, 0.0302 ± 0.0012, is larger than expected from models, perhaps due to the presence of a small core-boundary ellipticity. The millimetric data could solve this problem by exhibiting smaller periodic terms allowing the separation of the k_2 from the core ellipticity effects. The millimetric data could also improve the separation of the competitive dissipative terms in the secular acceleration of the Moon, and the determination of the 2.9 years arbitrary libration of the Moon in longitude, which is probably due to core boundary effects.

In the field of geodynamics, the analysis of both LLR and VLBI data permitstet to determine the Earth's precession and nutation. LLR permits the faster determination of the Universal Time (Earth rotation). It allows us to determine the Earth's station co-ordinates and motion, the GM of the Earth, and to yield information about the exchange of angular momentum between the solid Earth and the atmosphere, as well as on the tides acceleration of the Moon. The millimetric data would improve the determination of the increase of the Moon's distance, presently 3.82 ± 0.07 cm/year, and consequently the estimation of the tides which cause the tidal acceleration responsible for the moving away of the Moon and the slowing down of the Earth's rotation.

LLR has contributed to solar system tests in gravitational theories and is at present the best way to test the principle of equivalence for massive bodies. Following Nordtvedt, violation of the principle of equivalence should cause the polarization of the Moon's orbit about the Earth-Moon centre of mass in direction of the Sun. Currently, LLR analysis gives the ratio of the gravitational mass M_G to the inertial mass M_I for the Earth (as compared to the Moon): $M_G/M_I - 1 = (2 \pm 5)\ 10^{-13}$, corresponding to $C_0\eta = -0.7 \pm 1.4$ cm or $\eta = -0.0005 \pm 0.0011$, where C_0 is the characteristic size of the polarized orbit elongation and η is the Nordtvedt coefficient. The above result can be interpreted as a test of the parameter β_R from the Parametrized Post-Newtonian, providing $\beta_R = 0.9999 \pm 0.0006$. The millimetric data could lead to a better than 10^{-4} precision of the β_R coefficient measuring a superposition of gravitational effects. A second important test is the measurement of the relativistic precession of the lunar orbit in agreement with the predictions of General Relativity of 0.9%. LLR also provides a test of a possible change in the gravitational constant G.

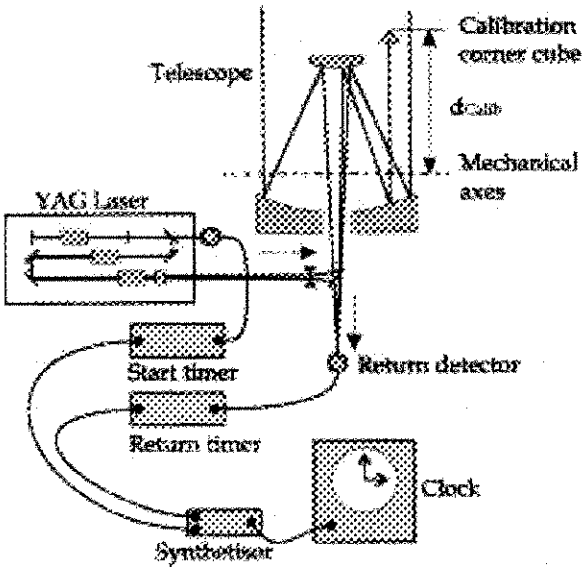

Fig. 1. OCA Lunar Laser Ranging facility

3. Experiment description

The experiment, as performed at OCA, is shown in Fig. 1. The YAG laser emits four short pulses at a rate of 10 Hz. The time intervals between the first and the second pulse, the third and the last one, are respectively: 1.6 ns, 4.1 ns and 5.7 ns. This temporal code, imagined by Jean-François Mangin, permits to deduce, without any ambiguity, the pulse position in the echo diagram. A telescope of 1.5 meter aperture collimates the laser beam in the lunar direction. A fraction of the photons coming from the laser output is sent onto a PIN photodiode. This detector is connected to a start timer giving the start time t_{Start} of the laser pulse. The photons coming from the Moon impinge a return detector. This return detector is connected to a return timer, similar to the start timer, giving t_{Return}. The time base of the timers is a caesium atomic clock. A corner cube, at the telescope output, returns a fraction of the emitted photons onto the return detector (Mangin 1982). This permits to calibrate the instrumentation. The arrival time of the calibration pulse on the return detector is t_{Calib}. This calibration information allows us to know accurately the transit time of the light pulse between the corner cube on the Moon and the calibration corner cube. The spatial reference of the LLR station is the crossing of the telescope mount axes. Finally, the distance between

this spatial reference and the target will be known if the distance between the cross axis and the calibration corner cube distance d_{Calib} is known (see Fig. 1). This distance is measured geometrically. The round trip travel time T_{Obs} of the light pulse between the spatial reference and the Moon corner cubes is

$$T_{\text{Obs}}(t_{\text{Start}}) = (t_{\text{Return}} - t_{\text{Start}}) - \langle t_{\text{Calib}} - t_{\text{Start}} \rangle + \frac{2d_{\text{Calib}} n_{\text{Air}}}{c} \quad (1)$$

where $\langle t_{\text{Calib}} - t_{\text{Start}} \rangle$ is the calibration mean value integrated over a period τ_{Calib}, n_{Air} is the air refraction index, and c is the light velocity. The mean value of the photon number coming from the Moon and detected per pulse by the return detector is of the order of 0.01. Thus, the return detector works in a single photon mode. Since the transit time of the return detection device depends on the number of received photons, the calibration will be valid if it is also performed in a single photon mode.

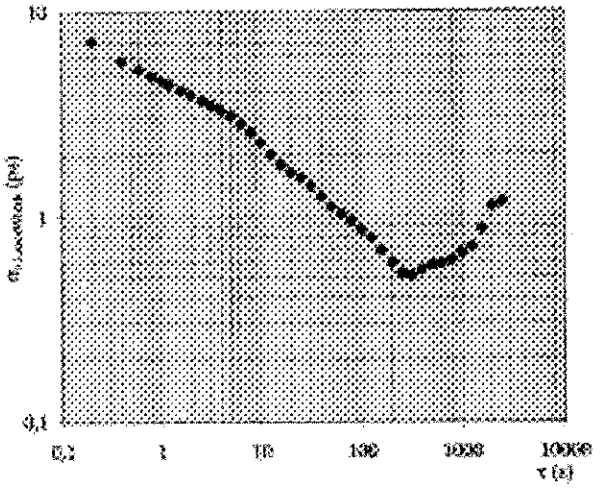

Fig. 2. Time stability of the laser pulse width. The time interval between two laser pulses is 0.2 s

4. Error budget

To perform a statistical analysis, we introduce the time interval T_{Residual} which is the difference between the measured time interval T_{Obs} given by Eq. (1) and the computed travel time T_{Comp}. The residual precision σ_{Residual} is defined by the root mean square of T_{Residual}, measured in stable conditions. Since the measurements are corrected by the term $\langle t_{\text{Calib}} - t_{\text{Start}} \rangle$ at a period τ_{Calib}, all the instrumental precisions have to be evaluated over a period τ_{Calib}. This condition concerns the start and the return detectors, the laser, and the timers. The accuracy of the measurement E_{Echoes} illustrates the error between the real distance and the measured distance. It depends on the precision of the measurement and on the unknown systematic errors. One obtains only an estimation of the accuracy. The measurements being degraded by some noises, which are time dependant, it is convenient to introduce the time stability $\sigma_x(\tau)$ of these measurements over a period τ. This can be computed by the Time variance TVAR (Allan et al. 1991). To evaluate the precision, the accuracy and the stability, we first present the different uncertainty sources involved in the lunar measurement.

4.1. Uncertainty sources

4.1.1. Laser

The laser characteristics are:

- type: YAG
- 4 pulses at a rate of 10 Hz
- λ = 532 nm and 1064 nm
- FWHM = 70 ps
- Energy: 75 mJ @ 532 nm; 75 mJ @ 1064 nm per pulse.

The mean value of the light pulse width is in the range of 70 ps. The shape of the pulse is Gaussian. The pulse width experiences some variations between 50 ps and 90 ps, caused by temperature inhomogeneities in the laser cavity. These variations are only encountered during the warm-up of the laser and a stable regime is obtained after thirty minutes. The start detector response is sensitive to the variation of the pulse width since the detector receives a large amount of photons. The variation δt of the laser width introduces a shift equal to $\delta t/2$ between the pulse centre and the photo-detector electrical response. The laser width root mean square of about 50000 laser pulses, measured in stable conditions, is 9 ps. This quantity will introduce in the global error budget the term $\sigma_{\text{Laser Edge}} = 4$ ps rms. The return detector response is sensitive to the width of the laser pulse since it is working in a single photon mode. The term added to the error budget, deduced from the laser FWHM, is $\sigma_{\text{Laser Width}} = 30$ ps rms. Figure 2 shows the time stability of the pulse width. The time interval τ_0 between each measurement is 0.2 s. All these laser width measurements are performed with a streak camera Hamamatsu C1587.

4.1.2. Start detector

The start detector is an InGaAs photodiode of 80 μm aperture, coupled with a very fast comparator. The laser light is extracted for the start detection at the cavity output with a mono-mode fiber of 15 m length. The detection is performed on the infrared pulses. Since the green pulses are generated from the infrared ones by a second harmonic generation phenomenon in a nonlinear medium, there is no time variation between the infrared and the green pulses. The amount of photons impinging the start detector and

the configuration of the device permit to obtain an electrical response which is quite independent of the photon number: lower than 10 ps/octave. Some individual experiments have shown that the time precision $\sigma_{\text{Start Detector}}$ of the start detector is better than 5 ps.

4.1.3. Return detector

The return detector is an avalanche photodiode built by Silicon Sensor (SSOAD230H) working in Geiger mode (Ekstrom 1981); (Samain 1998). Its aperture is 230 μm. The photodiode break-down voltage is 140 V. The total voltage applied on the photodiode to detect the photons is 290 V. The detector operates at -40 °C. The quantum efficiency in Geiger mode is 0.2. Some workbench experiments have shown that the transit time experiences a variation versus the position of the light spot on the active surface of the detector. With r being the distance between the photodiode centre and the spatial point where the photon is absorbed, and $T_{\text{Return Detector}}(r)$ the transit time difference between the response obtained with a photon absorbed at the centre and the response obtained at a distance r, we have measured

$$T_{\text{Return Detector}}(r) = ar^2; a = 0.005 \text{ ps}/\mu\text{m}^2. \quad (2)$$

In the case where the light spot's radius is R, the transit time mean value $< T_{\text{Return Detector}} >$ is a function of the above equation and of the probability $P(r)$ that a photon is absorbed in a ring of width δr and of diameter r. We then have

$$P(r) = \frac{2r\delta r}{R^2} \quad (3)$$

and

$$\langle T_{\text{Return Detector}} \rangle = \int_0^R \frac{2r\mathrm{d}r}{R^2} ar^2 = \frac{1}{2}aR^2. \quad (4)$$

Experimentally, we found, with $R = 115$ μm, $\langle T_{\text{Return Detector}} \rangle = 39$ ps (the above computation gives 33 ps).

The best time precision $\sigma_{\text{Return Detector}}$ of the photodiode is obtained with $r = 0$ and with a spot radius R as small as possible. Then, we have $\sigma_{\text{Return Detector}}$ $(r = 0, R = 20$ μm$) = 35$ ps. In the case where the whole active area of the photodiode is used we have $\sigma_{\text{Return Detector}}$ $(r = 0, R = 115$ μm$) = 50$ ps.

The size of the lunar return spot is determined by the optical configuration and by the atmospheric turbulence. The seeing, which roughly varies from 1″ to 7″, modifies the spot size from 50 to 200 μm and the return detector precision $\sigma_{\text{Return Detector}}$ lies in an interval of 35–50 ps rms.

4.1.4. Timers

The timers were built by Dassault Electronique, a French company, for the OCA Lunar Laser ranging station. These timers were also designed to perform a Time Transfer by Laser Link experiment (under development at OCA and CNES, French space agency) with some performances improved by two orders of magnitude as compared to the current time transfer techniques (Fridelance et al. 1997). The time base of both timers, generated from a 10 MHz signal, is performed by a single synthesizer also designed by Dassault Electronique. The frequency time base of the timers is 200 MHz. The time precision σ_{Timer} of the timer is 5 ps and the resolution is 1.2 ps. The linearity error is of the order of 1 ps without any table correction. The time stability of the timer coupled within the synthesizer is 8 fs over 1000 s ($\tau_0 = 400$ μs). The time drift in a laboratory environment is below 5 ps over two months. The sensitivity in temperature is 0.5 ps per degree.

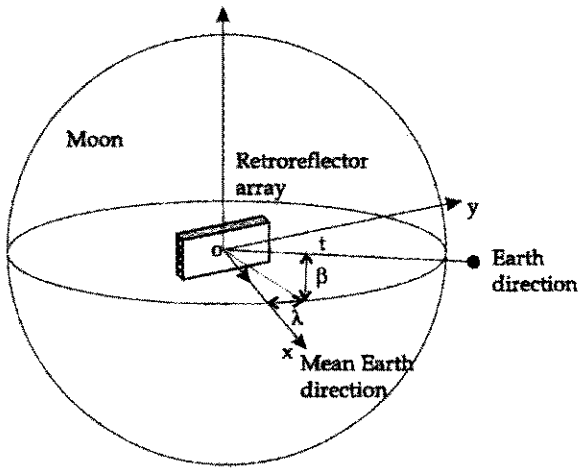

Fig. 3. Retroreflector orientation. The reflection point precision depends on the angle between $\boldsymbol{n}$ and $\boldsymbol{Ot}$

4.1.5. Retroreflector array orientation

Since the return detection operates in a single photon mode, an orientation difference between the normal axis of a retroreflector array $\boldsymbol{n}$ and the axis defined by the direction (retroreflector array, telescope) will introduce a dispersion in the measurements. This orientation difference depends on the lunar libration and on the initial orientation of the panel as compared to the mean orientation of the Earth centre as seen from the Moon ($\boldsymbol{Ox}$) (see Fig. 3). This latter is estimated at $\pm 1°$ for the Apollo retroreflectors and at $\pm 5°$ for the Lunakhod ones. The reflection point will be known with a certain precision which we expressed in time as $\sigma_{\text{Retroreflectors}}$. For simplification, one considers that the retroreflector array is located at the centre of the Moon. The vector $\boldsymbol{Ot}$ defines the instantaneous direction of the Earth telescope as seen from the Moon's centre. At a given date, the orientation $\boldsymbol{Ot}$, as compared to the mean direction $\boldsymbol{Ox}$, is given by the libration longitude

λ and the libration latitude β. The dispersion would be proportional to the angle $(\widehat{Ot}, \widehat{Ox})$ if the panel were symmetrical. This can be applied to the retroreflectors Apollo XI and XIV which are square. Then,

$$\sigma_{\text{Retroreflector}} = \frac{2D \sin(a \cos(\cos\beta \cos\lambda))}{c} \frac{1}{2\sqrt{3}} \quad (5)$$

where D is the equivalent size of the panel. The term $\frac{1}{2\sqrt{3}}$ is introduced to obtain a rms precision, since the probability to obtain a return from a given corner cube of the panel does not depend on the location of the panel. For the Lunakhod and Apollo XV panels, the direction of the panel major axis p has to be taken into account in the dispersion computation. One defines L as the largest size of the panel (in the direction p) and l as the smallest. Approximating that the equivalent size D in Eq. (5) varies between L and l according to an ellipse, we get

$$D \approx \sqrt{L^2 \cos^2\theta + l^2 \sin^2\theta} \quad (6)$$

where θ is the sum of the angles between the projection of t on the planes $(\boldsymbol{yOz})$ and $(\boldsymbol{Oy})$, and the angle a between p and the plane $(\boldsymbol{xOy})$. One has

$$\theta = \frac{\sin\beta}{\cos\beta \sin\lambda} + \alpha. \quad (7)$$

The panel sizes are (Faller 1972); (Fournet 1972)

1040×630 mm^2 for Apollo XV
450×450 mm^2 for Apollo IX and XIV
440×190 mm^2 for Lunakhod 1 and 2

$\sigma_{\text{Retroreflectors}}$ lies in an interval from 0 to 350 ps rms for the larger retroreflectors (Apollo XV), and from 0 to 150 ps for the smallest. The correlation between the theoretical and the observed precisions on Apollo versus the lunar libration XV will be studied in the following (Sect. 4.2).

4.1.6. Noise

Some noise events can degrade the precision of the measurements. These noise events are introduced by photons coming from the Sun and by thermal triggering of the avalanche photodiode. The latter events can be neglected. When the retroreflector is in the lunar day, the measured noise frequency f_{Noise} is of about 2 MHz. On the contrary, in the lunar night the noise frequency is a few kHz. This noise depends on the field of view of the optics, the spectral width of the interferential filter placed in front of the detector, and the telescope aperture. The light events outside a temporal gate $\Delta t = 6\ \sigma_{\text{Residual}}$ are eliminated. The noise event number accumulated during an observation period T_{Obs} in this gate Δt is $f_{\text{Noise}}\ f_{\text{Shoot}}\ T_{\text{Obs}} \Delta t$, where f_{Shoot} is the laser rate (10 Hz). The noise events being random, the residual precision σ_{Residual} is given by

$$\sigma^2_{\text{Residual}} = k\sigma^2_{\text{Noise}} + (1-k)\sigma^2_{\text{Residual}'} \quad (8)$$

where k is the fraction between the noise events and the total events number inside the gate Δt. σ_{Noise} is the root mean square of the noise events taken in the gate Δt, and $\sigma_{\text{Residual}'}$ is the residual precision without any noise events. Since the noise is white, we have $\sigma_{\text{Noise}} = \frac{\Delta t}{2\sqrt{3}}$. The filtering at $\pm$ 3 sigma implies $\sigma_{\text{Noise}} = \sqrt{3}\sigma_{\text{Residual}}$. Finally, one gets

$$\sigma^3_{\text{Residual}} \cdot \frac{18 f_{\text{Noise}} f_{\text{Shoot}} T_{\text{Obs}}}{N_{\text{Residual}}} - \sigma^2_{\text{Residual}} - \sigma_{\text{Residual}} \frac{6\sigma^2_{\text{Residual}} f_{\text{Noise}} f_{\text{Shoot}} T_{\text{Obs}}}{N_{\text{Residual}}} + \sigma^2_{\text{Residual}'} = 0 \quad (9)$$

where N_{Residual} is the events number inside the gate Δt taken in the computation. Figure 4, which illustrates Eq. (9), allows us, for $T_{\text{obs}} = 600$ s, $f_{\text{Shoot}} = 40$ Hz, to evaluate the precision degradation versus the fraction $f_{\text{Noise}}/N_{\text{Residual}}$ for different $\sigma_{\text{Residual}'}$. In the case where $f_{\text{Noise}} = 2$ MHz, $N_{\text{Residual}} = 100$, and $\sigma_{\text{Residual}'} = 200$ ps, one gets $\sigma_{\text{Residual}} = 300$ ps. If f_{Noise} is in the kHz range, (lunar night and echoes obtained during the night), the precision degradation due to noise is not significant.

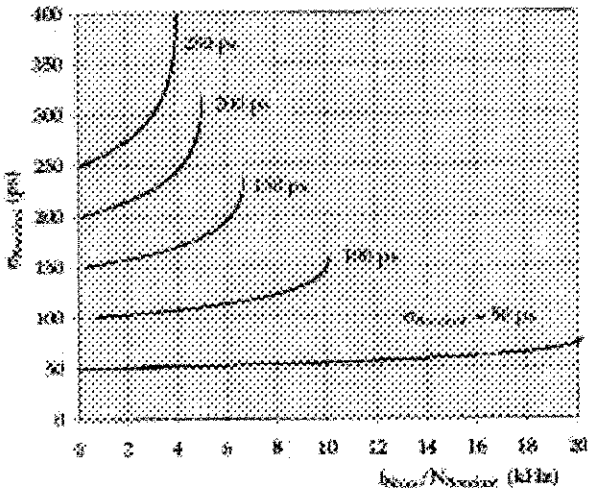

Fig. 4. Precision degradation versus the quantity $f_{\text{Noise}}/N_{\text{Residual}}$, for different values of $\sigma_{\text{Residual}'}$. Better is the time precision without any noise $\sigma_{\text{Residual}'}$, less sensitive to noise is the global precision σ_{Residual}

4.1.7. Time base

The time base of the timers is a commercial atomic clock HP 5071A. The frequency accuracy of this clock is better than 10^{-12}. The temporal error corresponding to the clock frequency error is of the order of $E_{\text{Clock}} = 3$ ps over 2.5 s. In the time interval $0.2 < \tau < 3$ s, the clock signal is perturbed with a flicker frequency modulation. The Allan variance root square $\sigma_{y.\text{Clock}}$ is

$$\sigma_{y.\text{Clock}} = 5\ 10^{-12} \tau^0;\ 0.2 < t < 3\ s. \quad (10)$$

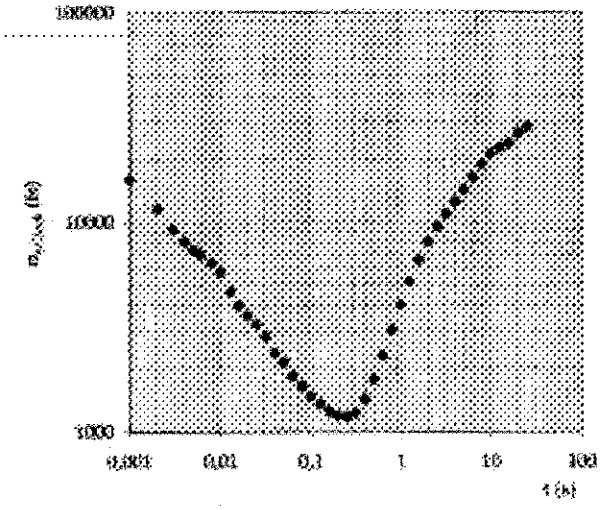

Fig. 5. HP 5071A – HP 5061A clocks time stability

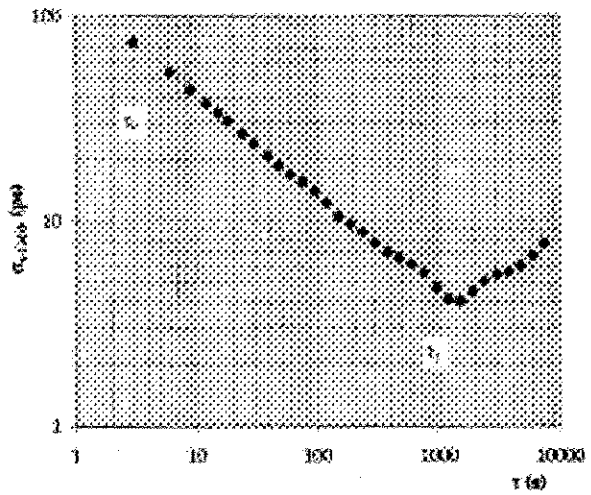

Fig. 6. LLR calibration time stability. Between τ_0 and τ_1, the calibration is perturbed by some white phase noise

These stability and accuracy data are provided by the constructor. After conversion into time variance (TVAR) one gets

$$\sigma^2_{x.\text{Clock}} = 0.645 \frac{\tau^2}{3} \sigma^2_{y.\text{Clock}} \tag{11}$$

where the coefficient 0.645 is the ratio of the modified Allan variance to the Allan variance. The temporal stability of the clock over 2.5 s will degrade the global precision of the measurement by $\sigma_{x.\text{Clock}}(\tau = 2.5\text{ s}) = 6$ ps. Figure 5 shows a time stability measurement of the HP 5071A and HP 5061A atomic clocks. The measured stability corresponds to the HP 5061A stability, and the time stability performance of the HP 5071A is probably better. Taking into account the measured global time stability we get $\sigma_{x.\text{Clock}}(\tau = 2.5\text{ s}) = 10$ ps.

4.1.8. Calibration

The distance between the corner cube used for the calibration and the LLR spatial reference (cross of the mechanical axis) is measured geometrically. The maximum error of this measurement is estimated at 3 mm. This error will introduce a systematic time error $E_{\text{Geometric}} = 10$ ps. The optical components of the telescope are tied together with some invar rods. Consequently, the variation in distance of the calibration path can be neglected.

The transit time sensitivity of the return detector versus the spatial position of the light spot on the detector will introduce an error in the distance measurement if the light spot of the calibration and the light spot of the lunar returns are located at different places or, if the spot sizes are different. The speed aberration, due to Earth and Moon rotation, combined with an eventual non alignment of the laser axis with the reception axis, can introduce an offset with regard to the centre of the photodiode of the order of 100 μm. This offset, expressed in time versus Eq. (2), gives $T_{\text{Return Detector}} = 50$ ps. A gelatine polarizer is placed on the calibration path to adjust the calibration level versus the telescope orientation. This polarizer acts also as a diffuser and broadens the calibration spot size which is then limited by the diaphragm. Combining the optical aberration and this diaphragm limitation, the spot radius of the calibration pulse is 100 μm, and $\langle T_{\text{Return Detector}} \rangle$ for the calibration is 25 ps. This magnification of the calibration spot size allows us to obtain a calibration information which is quite independent of the adjustment of the calibration spot position. As compared to $T_{\text{Return Detector}}$ an error of 25 ps can be introduced in the global error budget by this alignment problem. Another accuracy problem will be encountered if the voltage mean value applied on the return detector for the calibration echoes is different from the one used for the lunar echoes. The observed voltage difference is of the order of 3 V. Converted into time, this will introduce an error in the range of 15 ps. Finally, the phenomena introduced by the return detector degrade the accuracy measurement with a term $E_{\text{Calibration Detector}} = 65$ ps.

The echoes detected from the Moon are corrected with the term $\langle t_{\text{Calib}} - t_{\text{Start}} \rangle$. This mean value is computed from a set of dates, recorded over a time τ_{Calib}. The period τ_{Calib} should be deduced from the calibration time stability. The typical shape of this time stability is shown in Fig. 6. For τ between $\tau_0 = 0.5$ s and $\tau_1 = 1000$ s, one has some white phase noise ($\sigma_{x.\text{Calib}} = 5.1\ 10^{-11}\ \tau^{-1/2}$). The determination of the calibration mean value $\langle t_{\text{Calib}} - t_{\text{Start}} \rangle$ has to be computed from the larger time interval, τ_{Calib} less than τ_1, that is to say $\tau_{\text{Calib}} = \tau_1$. If it is computed from $\tau_{\text{Calib}} > \tau_1$, we would loose some information and on the contrary, if $\tau_{\text{Calib}} < \tau_1$,

the residuals will be perturbed by a useless white phase noise. Following this rule, the calibration correction will introduce a dispersion in the global error budget equal to $\sigma_{(\text{Calib-Start})} = 4$ ps.

4.1.9. The atmosphere

It is essential to know the air index on the travel path of the laser beam to take into account the delay introduced in the measurements (Herring 1992). This delay is computed from the Marini Murray model (Marini & Murray 1973). The computation uses some atmospheric measurements performed near the station. An error in the evaluation of the real air index value will introduce an accuracy problem. The accuracy $E_{\text{Atmosphere}}$ evaluated on the delay is 15 ps when the Moon is observed at an elevation of 90° (that is not possible in France) and 70 ps at 15°. An unknown air index variation on the laser beam path will degrade the precision of the measurement. The short term perturbation $0.5 < \tau < 1000$ s of the residual is a white phase noise (see Fig. 8). If the atmosphere has an effect on the measurement, this effect has a time constant lower than 0.5 s or greater than 1000 s. Some stellar interferometry experiments demonstrate that a phase correlation exists between two beacons a few tens of meters apart. The evolution of the phase between the beacons is a continuous function. The phase drift is lower than 100 wavelengths over 100 s. The corresponding time propagation difference between the beacons is then smaller than 0.1 ps. This interferometric measurements are relative (between the beacons) and do not give any information on the absolute time propagation of the light. Nevertheless, it seems improbable that the atmosphere exhibits an important air index variation at a spatial scale of a few tens of meters with a time scale lower than 0.5 s. Concerning the air index fluctuation over a period longer than 1000 s, Fig. 8 cannot yield any consistent information, since the observed flicker noise could be generated by some other sources (computation, clock, return detector, ...). Other experiments should be performed to improve our knowledge of the long term atmosphere comportment. In conclusion, the dispersion $\sigma_{\text{Atmosphere}}$ introduced by the atmosphere, computed over a period lower than 1000 s, will be small as compared to other dispersions and will be neglected in the global precision error budget.

4.2. Precision

The error budget for the precision, deduced from Eq. (1), is

$$\sigma^2_{\text{Residual}'} = \sigma^2_{\text{Start}} + \sigma^2_{\text{Return}} + \sigma^2_{(\text{Calib-Start})} + \sigma^2_{\text{Geometric}} \quad (12)$$

where $\sigma_{\text{Residual}'}$ is the residual precision without any noise. Taking into account all the elements intervening in the residuals, one gets

$$\sigma^2_{\text{Residual}'} = \sigma^2_{\text{Start Detector}} + \sigma^2_{\text{Laser Edge}} + \sigma^2_{\text{Timer}} + \sigma^2_{\text{Return Detector}} + \sigma^2_{\text{Laser Width}} + \sigma^2_{\text{Timer}} + \sigma^2_{x,\text{Clock}}(2.5\ s) + \sigma^2_{\text{Retroreflectors}} + \sigma^2_{(\text{Calib-Start})}. \quad (13)$$

As seen before, one has

- $\sigma_{\text{Laser Edge}} = 4$ ps: leading edge variation of the laser pulse
- $\sigma_{\text{Laser Width}} = 30$ ps: width of the light pulse
- $\sigma_{\text{Start Detector}} = 5$ ps and $\sigma_{\text{Return Detector}} = 50$ ps: start and return detector
- $\sigma_{\text{Timer}} = 5$ ps: electronic timer
- $\sigma_{x,\text{Clock}}(2.5\ \text{s}) = 10$ ps: time stability of the clock over a period of 2.5 s
- $\sigma_{\text{Retroreflectors}} = 0 - 350$ ps: retroreflector orientation
- $\sigma_{(\text{Calib-Start})} = 4$ ps: calibration.

Numerically, one gets: $\sigma_{\text{Residual}'} = 60$ ps in the case where the retroreflector dispersion is 0. This value corresponds to the better precision obtainable on the travel time of light pulses from Earth to Earth via the Moon. This time precision allows us to measure the Earth-Moon distance with a precision of 9 mm. This computation agrees with the calibration precision computed over τ_{Calib}. Among all the instrumental error sources, the main dispersion comes from the return detector. Figure 7 shows the residual precision σ_{Residual} obtained on the Apollo XV retroreflector and the theoretical precision taking into account the dispersion generated by the retroreflector array orientation $\sigma_{\text{Retroreflectors}}$. The precision is determined from the residual obtained since 1995 on the Apollo XV retroreflector array. σ_{Residual} is computed with the echoes accumulated over several hours in order to improve the

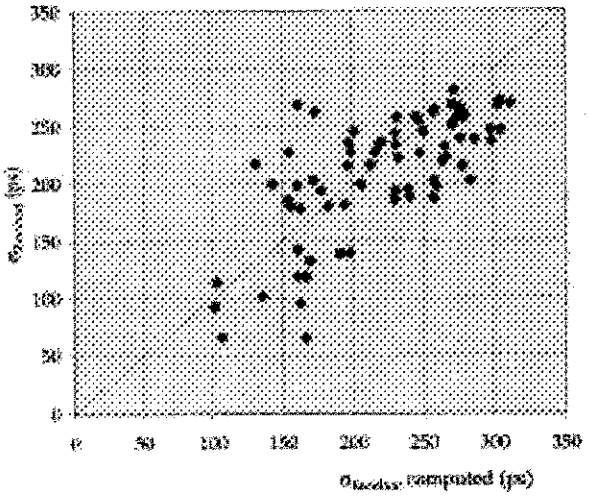

Fig. 7. Residual precision computed from the corner cubes array orientation and the intrinsic LLR performances versus the residual precision measured. Retroreflector: Apollo XV

error on the precision. To avoid any degradation of the precision due to the orbit determination, the residuals are fitted by a fourth order polynomial. The angle between the vector p and the plane (xOy) is fixed to 0. The normal axe of the retroreflector is supposed parallel to the mean Earth direction (Ox) (see Fig. 3). The good correlation between the theory and the measurements demonstrates that all the elements intervening in the precision error budget have been taken into account. This graph shows also that the precision of the Earth-Moon measurement is almost always limited by the retroreflector orientation. A future precision improvement of the LLR stations would be interesting if the echo numbers on the other retroreflector arrays (which are smaller than the Apollo XV ones) were increased.

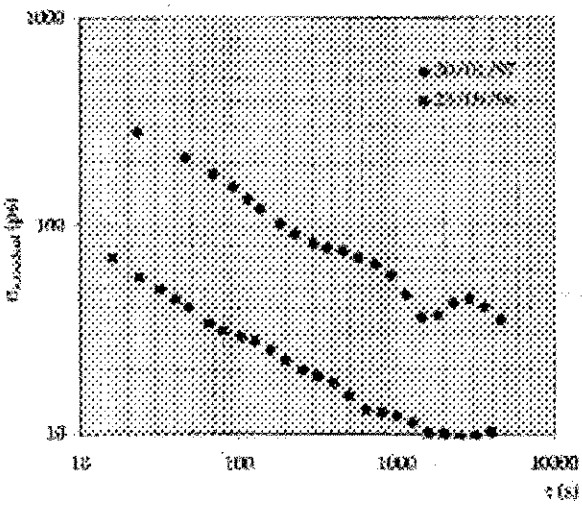

Fig. 8. Residual time stability computed from echoes obtained on Apollo XV. The normal point precision deduced from the 23/09/96 observation session is 10 ps (1.5 mm), and the best τ_{Residual} is 1500 s

4.3. Accuracy

The error sources intervening in the accuracy E_{Echoes} of the light pulses travel time from the Earth to the Earth via the Moon are:

- $E_{\text{Clock}} = 3$ ps: frequency clock accuracy
- $E_{\text{Geometrical}} = 10$ ps: accuracy of the geometrical distance of the calibration corner cube as compared to the reference point of the station
- $E_{\text{Calibration Detector}} = 65$ ps: accuracy of the return detector for the calibration
- $E_{\text{Atmosphere}} = 50$ ps: accuracy evaluation of the atmospheric delay
- $2\sqrt{3}\ \sigma_{\text{Residual}} = 220 - 1200$ ps: residual precision $65 < \sigma_{\text{Residual}} < 350$ ps.

One gets

$$E_{\text{Echoes}} = E_{\text{Clock}} + E_{\text{Geometrical}} + E_{\text{Calibration Detector}} + E_{\text{Atmosphere}} + 2\sqrt{3}\sigma_{\text{Residual}}. \quad (14)$$

Numerically, one obtains, in the best libration condition, $E_{\text{Echoes}} = 350$ ps, which corresponds to a Earth-Moon distance accuracy equal to 50 mm. The quantity $E_{\text{Echoes}}/2$ is an evaluation of the absolute value of the maximum difference between the round trip time deduced from one echo and the real distance. It illustrates the worst possible case to envisage. As we will see in the following chapter, the measurement accuracy can be improved by eliminating a fraction of the noise introduced by the residual precision. This is achieved by computing the mean value of many individual measurements.

4.4. Normal point

A normal point is the round trip time of the light pulse at a given time t from the spatial reference of the station to the retroreflector array computed from many individual echoes. This computation permits to decrease the computational time necessary for the scientific use of these data and to reduce the amount of data. For an integration period τ_{Normal} we have a set of observed round trip time intervals $T_{\text{Obs}}(i)$ at the date $t(i)$. We also have a set of computed round trip time intervals $T_{\text{Comp}}(i)$ at the same date $t(i)$. We compute the date mean value $\langle t \rangle$ from $t(i)$ and look for the nearest date $t(n)$ from $\langle t \rangle$. Corresponding to this date $t(n)$ one has a computed round trip time interval $T_{\text{Comp}}(n)$. The normal point T_{Normal}, giving the mean round trip time at the date $t(n)$ is

$$T_{\text{Normal}} = T_{\text{Comp}}(n) + \langle T_{\text{Obs}} - T_{\text{Comp}} \rangle . \quad (15)$$

This computation method has been introduced by Christian Veillet. Since the beginning of LLR, the determination of τ_{Normal} has been more or less arbitrarily fixed to ten minutes. To be sure that there is no information lost during the realization of a normal point, a time stability study of the measurement has to be performed. Figure 8 shows the residual time stability computed from two complete observation nights (23/09/96 and 30/01/97) on the Apollo XV retroreflectors. It appears that two kinds of noise are present in the data. For the best stability curve, one gets:

- $10 < \tau < 1500$ s: $\sigma_{x.\text{Residual}}(\tau) = 3\ 10^{-10}\ \tau^{-1/2}$ corresponding to a white phase noise
- $1500 < \tau < 5000$ s: $\sigma_{x.\text{Residual}}(\tau) = 10\ 10^{-12}\ \tau^{0}$ corresponding to a flicker phase noise.

In this case, the best choice for τ_{Residual} is 1500 s. The precision of the normal point computed over this period is $\sigma_{x.\text{Residual}}(\tau_{\text{Residual}} = 1500\text{ s}) = 10$ ps which corresponds to a distance precision equal to 1.5 mm. The accuracy of the normal point is improved as compared to the accuracy of each individual echo. One gets

$$E_{\text{Normal}} = E_{\text{Clock}} + E_{\text{Geometrical}} +$$

$$E_{\text{Calibration Detector}} + E_{\text{Atmosphere}} + 2\sqrt{3}\sigma_{x.\text{Residual}}(\tau_{\text{residual}}). \quad (16)$$

Numerically, for the 29/09/96, $E_{\text{Normal}} = 160$ ps (24 mm).

In practice, the period τ_{Residual} is not a constant. This way, to preserve all the information in the normal point, a time stability analysis is necessary. Another way is to set τ_{Calib} small enough so to be sure that no information has been eliminated. In this case, both the computational time and the amount of data will be raised. Furthermore, the accuracy and the precision of the normal point will not illustrate the best accuracy and precision available. In all cases, since information storage is today not a problem, the echoes should be saved without any filtering (one year of LLR echoes would represent only a few Mo).

5. Perspectives and conclusions

Some recent instrumental developments will allow us to improve both the stability and the accuracy of the distance measurements. The terms $E_{\text{Calibration Detector}}$ and $\sigma_{\text{Calibration Detector}}$ could be reduced by improving the Geiger voltage stability applied on the photodiode and by reducing the spot size of the light beam. We designed a device able to apply the Geiger voltage with a delay of the order of 10 ns having a voltage stability of 1 Vpp. The spot reduction could be achieved by increasing the optical magnification. Some optical components having adapted the equivalent focal and a sufficient aperture are today capable to obtain a spot size for both the calibration and the lunar echoes in the range of 100 μm. With these improvements, $E_{\text{Calibration Detector}}$ would be reduced to 10 ps, and $\sigma_{\text{Calibration Detector}}$ to 37 ps. These minor modifications will permit to obtain a residual precision $\sigma_{\text{Residual}} = 50$ ps as compared to the present 60 ps, and an accuracy on the normal point $E_{\text{Normal}} = 105$ ps (16 mm) as compared to 160 ps (24 mm). An improvement of the electronic devices used to shape the photodiode signals for the timer, and the utilisation of some high performance wire will permit to obtain a better time stability of the measurements. Figure 9 shows a workbench calibration time stability obtained when taking into account all the remarks listed above. The first plot is performed in a single photon mode, and the second in a multi-photons mode (about 1500 photons per pulse). The third plot represents the LLR calibration time stability as it is working today. The LLR calibration drift is of the order of 40 ps over three hours and less than 4 ps over the same time amount for the workbench experiment. The time stability of this workbench experiment obtained in multi-photons mode, is in the range of the laser width time stability (see Fig. 2). This means that, in this experiment, the main limitation comes from the laser. A temperature control improvement of the laser cavity or a reduction of the laser width would probably improve the limit. The performances obtained in multi-photons are interesting for the

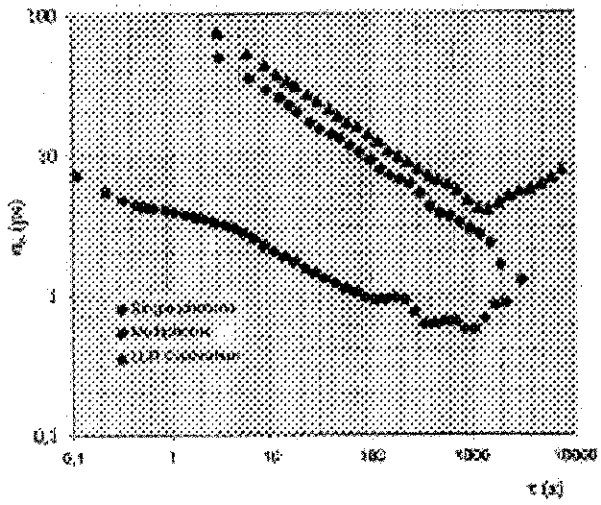

Fig. 9. LLR time stability as compared to the improved experiment in single photon and multi-photons modes. The best time stability curve is imposed by the laser width stability

satellite laser ranging but not for the LLR, since the return photon number is in the 0.01 range for the Moon. Converted into distance, this limit would permit to obtain some normal points integrated over $\tau = 300$ s with a precision of 0.1 mm. Of course, some other noises coming from the clock, the satellite corner cubes and the atmosphere, which are not taken into account here, will degrade this precision and it is difficult today to envisage the real precision that one would really observe. These stability improvement developments are first led at OCA for the Time Transfer by Laser Link (T2L2) experiment (Fridelance et al. 1997). The experiment will permit to transfer the temporal information of the new clock generation (Lea et al. 1994); (Salomon et al. 1996) without degrading the performances. In this context, the time stability of the laser station has to be better than the clock stability.

The main cause for dispersion on the Earth-Moon distance measurement comes from the orientation of the corner cubes array. The uncertainty added by this phenomenon in the measurement depends on the size of the retroreflector and the lunar libration. Statistically, since 1995, only 4.3% of the lunar echoes precision have been obtained with the intrinsic precision of the OCA LLR station. Due to the bad link budget, 88% of the normal point are obtained on the largest Apollo XV reflector, 5% and 6% on Apollo XI and XIV and only 1% on Lunakhod 2 which is the smallest one. As the average precision is proportional to the panel size, the improvement of the global precision will be obtained by increasing the number of echoes on the small panels. This could be obtained by increasing the photon number per pulse sent in the lunar direction, by increasing the laser shoot rate, by using adapted optics in order the decrease the spot size of the laser beam on the Moon, or by changing the laser

wavelength to improve the quantum efficiency of the return detector. As long as almost all the echoes are obtained only on the largest Apollo XV retroreflectors, a major improvement of the LLR station precision is not useful.

An important term is added by the atmosphere in the accuracy error budget. A preliminary work is led today by Nicolas Pelloquin to envisage a correction of the atmospheric delay deduced from some parameters directly measured by the retro-diffusion of the laser pulse sent to the Moon (Hauchecorne et al. 1992); (Argall & Jacka 1996). Another correction method, would be the two colours laser ranging (Lucchini 1996). In this method, the atmospheric delay information is extracted from the difference between the time propagation of light pulses having different wavelengths. Probably this information could not be extracted from the lunar echoes because the link budget is too bad, but from a satellite target located roughly in the direction of the Moon. The success of this method will depend on the spatial homogeneity of the atmosphere. The study of the two colour laser ranging is supported at OCA by Jean Gaignebet.

A continuous set of quality measurements is necessary to maintain and improve the ephemeris, the Earth's precession and nutation determination. The increased data density with an improved precision and accuracy will allow a better understanding of the Moon, the Earth, and the Earth-Moon system, and will also improve tests of gravitational physics and relativity.

Acknowledgements. The lunar libration ephemeris used in the computation of the residual precision has been provided by the NASA.

References

Allan D.W., Weiss M.A., Jespersen J.L., 1991, 45 Th Annual Symposium on Frequency Control
Argall P.S., Jacka F., 1996, Appl. Opt. 35, 2619
Chang R.F., Alley C.O., Currie D.G., Faller J.E., 1972, Space Res. XII, 246
Dickey J.O., Bender P.L., Faller J.E., 1994, Sci 265, 482
Ekstrom P.A., 1981, J. Appl. Phys. 52, 6974
Faller J.E., 1972, Space Res. XII, 235
Fournet M., 1972, Space Res. XII, 261
Fridelance P., Samain E., Veillet C., 1997, Exp. Astron. 7, 193
Hauchecorne A., Chanin M.L., Keckhut P., Nedeljkovic D., 1992, Appl. Phys. B 55, 29
Herring T.A., 1992, in: Munck J.D. and Spoelstra T.T., Refraction of Transatmospheric Signals in Geodey, p. 157
Lea S.N., Clairon A., Salomon C., Laurent P., et al., 1994, Phys. Scr. T51, 78
Lucchini C., 1996, Ph. D thesis, Université de Nice Sophia Antipolis
Mangin J.F., 1982, in: Wilson P. (ed.), 4 Th International Workshop on Laser Ranging Instrumentation
Marini J.W., Murray C.W., 1973, Nasa GSFC, X-591, 73
Nordvedt K., 1996, Phys. today, p. 26
Salomon C., Lemonde P., Laurent P., et al., 1996, in ESA Symposium Proceedings on Space Station Utilisation
Samain E., 1995, Ph. D. thesis, Université de Nice Sophia Antipolis
Samain E., 1998, Appl. Opt. 37
Veillet C., 1987, La Recherche 18, 394
Veillet C., Mangin J.F., Torre J.M., 1993, Contr. space Geodesy Geodyn. 25, 189-198
Williams J.G., Newhall X.X., Dickey J.O., 1996, Phys. Rev. 53, 6730-6739